

ESTIMATING THE FIRST-LIGHT TIME OF THE TYPE IA SUPERNOVA 2014J IN M82

WEIKANG ZHENG^{1,2}, ISAAC SHIVVERS¹, ALEXEI V. FILIPPENKO¹, KOICHI ITAGAKI³, KELSEY I. CLUBB¹, ORI D. FOX¹,
MELISSA L. GRAHAM¹, PATRICK L. KELLY¹, AND JON C. MAUERHAN¹,

Draft version February 11, 2014

ABSTRACT

The Type Ia supernova (SN Ia) 2014J in M82 ($d \approx 3.5$ Mpc) was serendipitously discovered by S. Fossey's group on 2014 Jan. 21 UT and has been confirmed to be the nearest known SN Ia since at least SN 1986G. Although SN 2014J was not discovered until ~ 7 days after first light, both the Katzman Automatic Imaging Telescope at Lick Observatory and K. Itagaki obtained several predisccovery observations of SN 2014J. With these data, we are able to constrain the object's time of first light to be Jan. 14.75 UT, only 0.82 ± 0.21 d before our first detection. Interestingly, we find that the light curve is well described by a varying power law, much like SN 2013dy, which makes SN 2014J the second example of a changing power law in early-time SN Ia light curves. A low-resolution spectrum taken on Jan. 23.388 UT, ~ 8.70 d after first light, shows that SN 2014J is a heavily reddened but otherwise spectroscopically normal SN Ia.

Subject headings: supernovae: general — supernovae: individual (SN 2014J)

1. INTRODUCTION

Type Ia supernovae (SNe Ia; see Filippenko 1997 for a review of SN classification) are used as standardizable candles and therefore have many important applications, including measurements of the changing expansion rate of the Universe (Riess et al. 1998; Perlmutter et al. 1999). However, our understanding of the progenitor systems and explosion mechanisms of SNe Ia remains substantially incomplete. It is well accepted that SNe Ia are the product of the thermonuclear explosions of C/O white dwarfs (Hoyle & Fowler 1960; Colgate & McKee 1969; see Hillebrandt & Niemeyer 2000 for a review), but early discovery and detailed observations are essential in order to determine the exact nature of the progenitor system and the details of the explosion process. Fortunately, with the modern telescopes and techniques now being used in searches for SNe, a number of recent SNe Ia have been discovered when quite young and have been studied in detail. Examples include SN 2009ig (Foley et al. 2012), SN 2011fe (Nugent et al. 2011; Li et al. 2011), SN 2012cg (Silverman et al. 2012a), SN 2012ht (Yamanaka et al. 2014), and SN 2013dy (Zheng et al. 2013; hereafter Z13).

Before SN 2014J, the nearest SN Ia detected in the modern age was SN 1986G in NGC 5128 (distance $d = 3.8 \pm 0.1$ Mpc; Harris et al. 2010), or perhaps SN 1972E in NGC 5253 ($d = 2.5$ – 8.0 Mpc, with a mean of ~ 3.8 Mpc; e.g., Phillips et al. 1992; Sandage & Tammann 1975; Della Valle & Melnick 1992; Branch et al. 1994; Sandage et al. 1994). SN 2011fe, another SN Ia found fewer than 3 yr ago, occurred in the nearby galaxy M101 ($d = 6.4 \pm 0.7$ Mpc; Shappee & Stanek 2011). The newly discovered SN 2014J in M82 ($d = 3.5 \pm 0.3$ Mpc; Karachentsev & Kashibadze 2006) is much closer than SN 2011fe, and it also appears to be slightly closer than SN 1986G or SN 1972E (but the latter's large distance uncertainty precludes an exact comparison). This means

that SN 2014J offers researchers a unique opportunity to study a nearby SN Ia in detail.

In this *Letter* we present our predisccovery photometric observations of SN 2014J along with an optical spectrum taken just two days after the discovery was reported. We include an analysis of these data and compare the early-time light curve of SN 2014J with that of SN 2013dy, another SN Ia found when it was very young.

2. OBSERVATIONS AND DATA PROCESSING

SN 2014J was serendipitously discovered by astronomer Stephen J. Fossey and a team of his students on Jan. 21.805 (UT dates are used herein) with a 0.35 m telescope at the University of London Observatory (Fossey et al. 2014). A number of predisccovery observations including detections and nondetections were reported after the discovery information was posted (e.g., Fossey et al. 2014; Ma et al. 2014; Denisenko et al. 2014). Among these reports, the earliest broadband detection is from the ROTSE team (Fossey et al. 2014), on Jan. 15.378. After this *Letter* was submitted, Goobar et al. (2014) also reported an iPTF detection in an H α image taken on Jan. 15.18.

SN 2014J was also observed by the 0.76 m Katzman Automatic Imaging Telescope (KAIT) as part of the Lick Observatory Supernova Search (LOSS; Filippenko et al. 2001). The host galaxy, M82, was monitored by KAIT with an average cadence of 2 days (Zheng et al. 2014) before the reported discovery. The supernova is clearly detected in images taken on Jan. 16.381 with no detection on Jan. 14.365 (unfiltered limiting magnitude > 18.9). We measure its J2000.0 coordinates to be $\alpha = 09^{\text{h}}55^{\text{m}}42.108^{\text{s}}$, $\delta = +69^{\circ}40'25''.87$, with an uncertainty of $0''.20$ in each coordinate. SN 2014J is $55''.2$ west and $20''.0$ south of the somewhat ill-defined nucleus of M82. It is unfortunate that KAIT/LOSS did not automatically discover SN 2014J when first observed by KAIT. The paucity of suitable stars in the field, as well as the bright and complex background light from M82, confounded our image-subtraction and object-identification pipeline.

Several images of SN 2014J were also taken by K. Ita-

arXiv:1401.7968v2 [astro-ph.HE] 10 Feb 2014

¹ Department of Astronomy, University of California, Berkeley, CA 94720-3411, USA.

² e-mail: zwk@astro.berkeley.edu .

³ Itagaki Astronomical Observatory, Teppo-cho, Yamagata 990-2492, Japan.

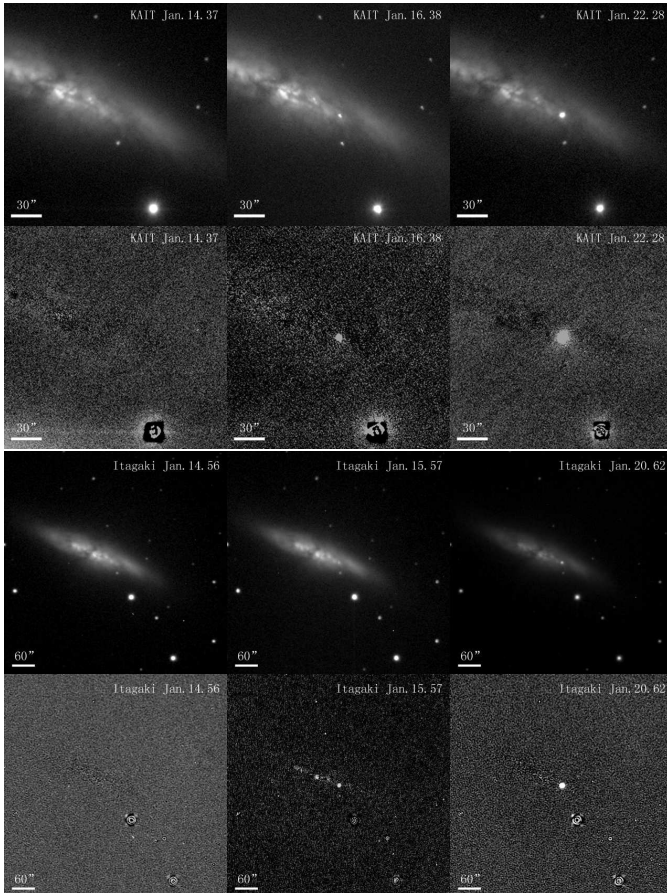


FIG. 1.— Top row: KAIT images of SN 2014J at three different epochs, including the latest KAIT nondetection on Jan. 14.37. Second row: KAIT residual images at the same epochs after subtraction. Third and bottom rows: Same as the top two rows, but for the Itagaki images, including the latest nondetection on Jan. 14.56. SN 2014J is located at the center of each image.

gaki, with a daily cadence from Jan. 13 to Jan. 17, using a 0.5 m telescope at the Itagaki Astronomical Observatory, Japan. The object is clearly detected in an image taken on Jan. 15.571, with no detection in an image from Jan. 14.559 (unfiltered limiting magnitude > 18.0). These data are used together with KAIT observations to perform a joint analysis, constraining the time of first light⁴ of SN 2014J. Both the KAIT and Itagaki prediscovery data were taken in unfiltered bands, while our multi-filter observations began only after discovery; thus, here we focus our analysis on the early unfiltered light curve.

All KAIT images were reduced using our image-reduction pipeline (Ganeshalingam et al. 2010), and we similarly processed and reduced all of the Itagaki images. In order to remove the host-galaxy contribution, we applied the same image-subtraction procedure to both KAIT and Itagaki images using a galaxy template image

⁴ Throughout this *Letter* we refer to the time of first light instead of explosion time because the SN may exhibit a “dark phase” lasting hours to days between the moment of explosion and the first emitted light (e.g., Rabinak, Livne, & Waxman 2012; Piro & Nakar 2012, 2013). We define the time of first light to be the time at which the luminosity of the SN is exactly zero in our model. As noted by Riess et al. (1999), “In principle, the initial luminosity is that of a white dwarf ($M_B = 10\text{--}15$ mag), but at the observed speed of the rise, the brightening from zero to a white-dwarf luminosity requires less than 1 s.”

taken with each telescope before the SN explosion. Figure 1 shows several examples of both KAIT and Itagaki images before and after subtraction, with SN 2014J located at the center of each image. Point-spread-function photometry was then performed using DAOPHOT (Stetson 1987) from the IDL Astronomy User’s Library⁵. The SN instrumental magnitudes have been calibrated to two nearby stars from the USNO B1.0 catalog: S1 with $R2 = 15.45$ mag and J2000 coordinates $\alpha = 09^{\text{h}}55^{\text{m}}25.2^{\text{s}}$, $\delta = +69^{\circ}41'21''.8$; S2 with $R2 = 15.09$ mag and J2000 coordinates $\alpha = 09^{\text{h}}55^{\text{m}}46.1^{\text{s}}$, $\delta = +69^{\circ}42'01''.8$.

For nondetections, we present an upper-limit magnitude (3σ). Owing to the complicated background light from M82, it is inappropriate to measure the image noise directly from the original image. However, the host-galaxy background structure is mostly absent after subtraction (as shown in Fig. 1). We therefore measure the standard deviation in the residual image at several positions around SN 2014J and use these to derive a 3σ upper limit on the object’s brightness and its uncertainty for each image. This is further cross-checked by simulation: we inject a simulated star signal (3σ of sky noise) into the nondetection images at the SN position, perform the same subtraction procedure, and measure the magnitude of the simulated star in residual images using aperture photometry. In 100 simulation trials, we are able to recover a majority ($> 95\%$) of the measurements with a mean magnitude value within 0.1 mag of our reported limiting magnitude.

Our analysis includes unfiltered observations from two separate telescopes and cameras, so it is necessary to measure any possible offset between KAIT and Itagaki magnitudes before beginning a joint analysis. Since both are unfiltered, the response of each system is dominated by the CCD quantum efficiency (QE). KAIT uses a MicroLine 77 camera from Finger Lakes Instrumentation⁶ (chip model E2V CCD77-00-BI-IMO), with a QE curve that reaches half-peak values at ~ 3800 and ~ 8900 Å. Mr. Itagaki uses a BN-83E camera manufactured by Bitran⁷ (chip model KAF-1001E), with a QE curve that reaches half-peak values at ~ 4100 and ~ 8900 Å. These response curves, and therefore the effective passbands of the two systems, are very similar. However, we can directly check by comparing photometry of isolated field stars that are present in both datasets. We did this for more than 30 stars in 4 different fields (including the SN 2014J field) that have recently been observed by both KAIT and Itagaki. We find that, overall, the unfiltered magnitudes measured from KAIT and Itagaki have a systematic offset of only 0.02 mag and a scatter of 0.02 mag. These stars exhibit a range of more than 0.9 mag in $B - R$ color, so we expect color-dependent difference between the two photometric systems to be small. Figure 2 shows a detailed magnitude comparison between the two systems, and Table 1 lists the raw photometry for both datasets. Before performing our joint analysis, we transform the Itagaki data into the KAIT magnitude system by subtracting 0.02 mag.

An optical spectrum of SN 2014J was obtained on Jan 23.388, ~ 8.70 d after first light, with the Kast dou-

⁵ <http://idlastro.gsfc.nasa.gov/>

⁶ <http://www.flicamera.com/index.html>

⁷ <https://www.bitran.co.jp/>

TABLE 1
 UNFILTERED PHOTOMETRY OF SN 2014J

MJD	UT	Mag	1 σ Error	Telescope
56667.4384	Jan. 10.4384	>18.2	-	KAIT
56671.3653 ¹	Jan. 14.3653	>18.9	-	KAIT
56673.3804	Jan. 16.3804	13.38	0.04	KAIT
56673.3811	Jan. 16.3811	13.37	0.04	KAIT
56675.3468	Jan. 18.3468	12.24	0.07	KAIT
56675.3471	Jan. 18.3471	12.21	0.04	KAIT
56675.3474	Jan. 18.3474	12.17	0.06	KAIT
56677.4528	Jan. 20.4528	11.27	0.08	KAIT
56677.4535	Jan. 20.4535	11.22	0.11	KAIT
56679.2793	Jan. 22.2793	10.73	0.04	KAIT
56679.4556	Jan. 22.4556	10.59	0.25	KAIT
56680.3441	Jan. 23.3441	10.39	0.09	KAIT
56680.3521	Jan. 23.3521	10.36	0.04	KAIT
56680.3852	Jan. 23.3852	10.41	0.07	KAIT
<hr/>				
56670.5914	Jan. 13.5914	>17.9	-	Itagaki
56671.5588	Jan. 14.5588	>18.0	-	Itagaki
56672.5705	Jan. 15.5705	14.01	0.03	Itagaki
56673.6414	Jan. 16.6414	13.28	0.06	Itagaki
56674.6124	Jan. 17.6124	12.67	0.13	Itagaki
56676.6179	Jan. 19.6179	11.58	0.06	Itagaki
56677.6205	Jan. 20.6205	11.24	0.05	Itagaki

¹ Coadd of 3 individual images.

ble spectrograph (Miller & Stone 1993) on the Shane 3 m telescope at Lick Observatory. The 2'' wide slit was aligned along the parallactic angle to minimize the effects of atmospheric dispersion (Filippenko 1982). The spectrum was reduced following standard techniques and was flux calibrated through observations of appropriate spectrophotometric standard stars (e.g., Silverman et al. 2012b). We deredshift it into the rest frame of M82 using $v = 203 \text{ km s}^{-1}$ (de Vaucouleurs et al. 1991). We correct for reddening due to Milky Way dust along the line of sight using the $R_V = 3.1$ reddening law of Cardelli, Clay-

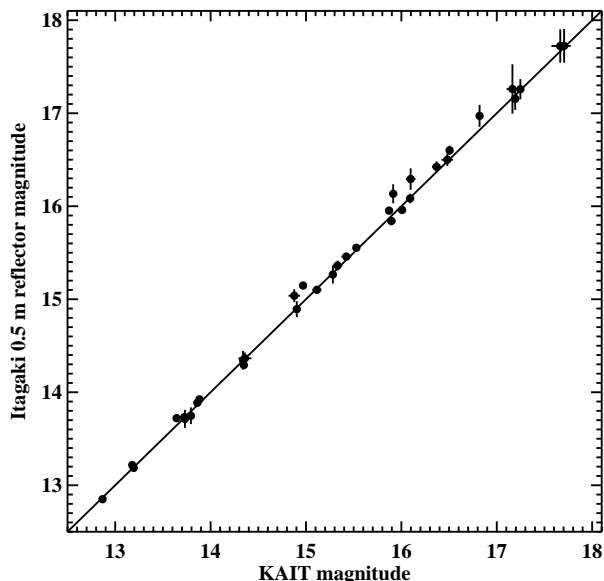


FIG. 2.— Comparison of the unfiltered KAIT and Itagaki magnitude systems for stars from 4 different fields observed by both telescopes at 4–15 different epochs. The solid line represents equivalence between the two systems. We find that the Itagaki magnitudes are systematically larger (fainter) by ~ 0.02 mag by measuring the median value of the differences.

ton, & Mathis (1989), adopting $E(B-V)_{\text{MW}} = 0.14$ mag (Schlafly & Finkbeiner 2011). In addition, SN 2014J is substantially obscured by dust in the host galaxy, M82. The very strong Na I absorption lines imparted on the spectrum by the interstellar medium (ISM) in M82 are saturated, and they exhibit total equivalent widths of 2.4 Å and 2.7 Å for D1 and D2, respectively (Cox et al. 2014; Polshaw et al. 2014). These values are well beyond the range where commonly used empirical relations for determining reddening are valid (Poznanski et al. 2013), making any sort of accurate host-galaxy reddening correction difficult at this time.

3. ANALYSIS AND RESULTS

3.1. Light Curves

Figure 3 shows our unfiltered light curves of SN 2014J, with KAIT data in pink and Itagaki data in blue. Our first detection of SN 2014J comes from an Itagaki image taken Jan. 15.571 (14.01 mag), followed by a KAIT detection on Jan. 16.381 (13.37 mag). Our latest nondetection comes from an Itagaki image taken Jan. 14.559 (>18.0 mag), with a KAIT nondetection from three coadded images at a mean time of Jan. 14.365 (>18.9 mag). These deep nondetections (more than 4 mag deeper than the first detection) within a single day of the first detection allow us to put a very tight constraint on the time of first light.

To determine the first-light time, one can assume that the SN luminosity scales as the surface area of the expanding fireball, and therefore increases quadratically with time ($L \propto t^2$, commonly known as the t^2 model; e.g., Arnett 1982; Riess et al. 1999). The t^2 model provides a good fit for several SNe Ia with early observations (e.g., SN 2011fe, Nugent et al. 2011; SN 2012ht, Yamanaka et al. 2014). We applied this model to the joint dataset from both KAIT and Itagaki, finding a poor fit (with χ^2 per degree of freedom of 1.73); the data imply a steeper power-law index. We therefore free the index of the power law and obtain a best-fit value of 2.89 ± 0.27 ($\chi^2/\nu = 0.26$), with a corresponding first-light time of Jan. 11.88, or 3.56 ± 0.58 d before our first detection.

Though the simple power-law model fits the detected light curve well (dashed black line in Fig. 3), it is strongly at odds with both the KAIT and Itagaki nondetections. The very deep nondetection limit requires the first-light time to be much closer to our first detection point, and a rapid increase in brightness (more than 4 mag) within a short time (one day) therefore yields a different power-law index. This is very similar to the case of SN 2013dy, which also showed a very rapid rise (the brightness of SN 2013dy increased more than 2 mag within the first 0.5 d). Hence, in a manner similar to our work on SN 2013dy (Z13), as well as to models widely used for observed gamma-ray burst afterglows (e.g., Zheng et al. 2012), we adopt a broken power-law model with a variable index for SN 2014J:

$$f = \left(\frac{t-t_0}{t_b}\right)^{\alpha_1} \left[1 + \left(\frac{t-t_0}{t_b}\right)^{s(\alpha_1-\alpha_2)}\right]^{-1/s}, \quad (1)$$

where f is the flux, t_0 is the first-light time, t_b is the break time, α_1 and α_2 are the power-law indices before and after the break (respectively), and s is a smoothing parameter.

In Z13, we were able to constrain the value of α_1 with a very early detection of SN 2013dy; sadly, we do not have a similarly early detection of SN 2014J. However, we use two methods to obtain quite narrow limits on the first-light time with the existing data. In Method 1, we treat the latest nondetection as a marginal “real detection,” yielding an effective upper limit on the value of α_1 . Assuming our broken power-law model applies back to the time of first light, it also provides a lower limit on this time. Based on this assumption, and setting the time of our first detection to $t = 0$, our best fit gives $t_0 = -1.03$ d, $t_b = 2.62 \pm 0.22$ d, $s = -36.9 \pm 12.3$, $\alpha_1 = 0.97 \pm 0.11$, and $\alpha_2 = 1.98 \pm 0.07$ ($\chi^2/\nu = 0.16$). This implies that first light occurred on Jan. 14.54, and the fit is shown by the solid red line in Figure 3. In Method 2, we assume that the very early rise of SN 2014J was similar to that of SN 2013dy. The best-fit α_1 value found for SN 2013dy was 0.88 ± 0.07 (Z13). To place a conservative upper limit on the first-light time of SN 2014J, we adopt $\alpha_1 = 0.67$, the α_1 value (3σ) from SN 2013dy. We find a best-fit model with $t_0 = -0.61$ d, $t_b = 2.20 \pm 0.12$ d, $s = -202.8 \pm 67.6$, $\alpha_1 = 0.67$ (fixed during fitting), and $\alpha_2 = 1.82 \pm 0.07$ ($\chi^2/\nu = 0.17$). This implies that first

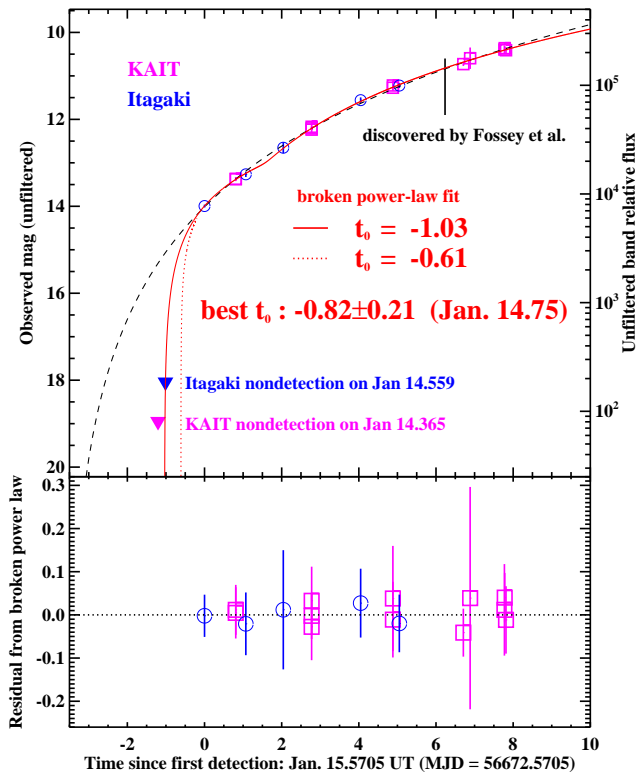


FIG. 3.— The top panel shows a broken power-law fit to the unfiltered light curve of SN 2014J with two different methods. Method 1 (solid red line) marks a lower bound on the date of first light by assuming that the latest nondetection (filled blue triangle) is a marginal “real detection” during fitting. Method 2 (dotted red line) marks an upper bound on the date of first light by adopting the 3σ limit for α_1 as fit from SN 2013dy, assuming that SN 2014J and SN 2013dy exhibited similar rise rates at very early times. See text for more details. The dashed black line is the best-fit result for a single power-law model, shown here for comparison. The bottom panel shows the residuals for Method 1. Our best estimate of the time of first light for SN 2014J is Jan. 14.75, or 0.82 ± 0.21 d before our first detection.

light occurred on Jan. 14.96, and the fit is shown by the dotted red line in Figure 3.

As shown above, the best fits for the $t^{2.89}$ model and the two broken power-law models are much better than the t^2 model. The χ^2/ν value for the $t^{2.89}$ model and the two broken power-law models are comparable, but a simple χ^2/ν analysis does not take into account the strong constraints from our nondetections, which rule out a simple power-law model. We therefore favor the broken power-law model.

Our two methods constrain the time of first light to be somewhere between 1.03 d and 0.66 d before our first detection. We adopt, as our best estimate, the mean of these two values: Jan. 14.75, or 0.82 ± 0.21 d before our first detection. Both the iPTF-H α and ROTSE detections are after, and thus consistent with, our derived first-light time (by 0.43 d and 0.63 d, respectively). This makes SN 2014J one of the earliest detected SNe Ia, along with SN 2013dy (0.10 d after first light; Z13), SN 2011fe (0.46 d; Nugent et al. 2011), and SN 2009ig (0.71 d; Foley et al. 2012).

The extremely rapid rise in the first day of SN 2014J’s light curve reinforces several of the conclusions obtained by Z13 when studying SN 2013dy, showing that the t^2 model is not sufficient for every SN Ia. (1) Within the first day after first light, some SNe Ia exhibit a very rapid increase in brightness, in the case of SN 2014J becoming more than 4 mag brighter in a single day. Actually observing this very rapid rise is a challenge given the very short timespan over which it occurs. (2) Some SN Ia light curves are best described by power laws with an exponent not equal to 2 (see also Piro & Nakar 2012). (3) The best-fit power-law exponent likely varies with time. With SN 2014J, we add to the mounting evidence that the t^2 model has worked for previous SNe Ia only because observations constraining the shape of the light curve at very early times were rare. The early-time light curves of SN 2013dy and SN 2014J demonstrate that a varying power-law exponent may be a common phenomenon in the light curves of very young SNe Ia, and that SNe Ia are likely more complex than the simple fireball model assumes.

The physical explanation for the varying exponent of SNe Ia is still unclear. Perhaps the very early fireball exhibits significant changes in either the photospheric temperature or the velocity during expansion, or the fireball input energy may change owing to the geometric structure of the Ni⁵⁶ distribution in outer layers. Another possibility is that the very early light curve may include some contribution from the shock-heated cooling emission after shock breakout, although this phenomenon is predicted to exhibit a power-law index of 1.5 ($f \propto t^{1.5}$; see Eq. 3 of Piro & Nakar 2013), not in good agreement with the values observed in SN 2013dy and SN 2014J.

3.2. Optical Spectra

Our Lick spectrum taken on Jan. 23.39 shows that SN 2014J is a spectroscopically normal SN Ia showing some high-velocity features and strong dust reddening, as noted by others (e.g., Cao et al. 2014). The analysis above indicates that this spectrum was taken ~ 8.7 d after first light. Note the prominent narrow absorption features produced by the host-galaxy ISM: two Ca II lines near 3950 Å and the Na I line near 5900 Å. We classify

the spectrum with the SuperNova IDentification code using an enhanced set of spectral templates (SNID; Blondin & Tonry 2007; Silverman et al. 2012b), which indicates a 100% match with premaximum SN Ia spectra ($\sim 90\%$ match to the SN Ia-norm subtype and $\sim 10\%$ match to the SN Ia-99a subtype).

As mentioned in § 2, it is difficult to determine the exact amount of reddening produced by the host galaxy, M82. However, Polshaw et al. (2014) suggest that the early-time light curve of SN 2014J indicates a total $E(B - V) \lesssim 0.8$ mag. Thus, for visual comparison only, we deredden our spectrum of SN 2014J to account for a dust contribution from M82 of $E(B - V)_{\text{M82}} = 0.66$ mag, assuming the same dust-law parameterization as described in §2 (in addition to the already-applied correction for Milky Way extinction). We then use SYN++/SYNAPPS (Thomas et al. 2011) to fit a simple parameterized SN Ia model to the dereddened spectrum. We obtain a good fit using only ions commonly found in SN Ia spectra: O I, Na I, Mg II, Si II, Si III, S II, Ca II, Fe II, Fe III, and Ni II. We see little evidence for the presence of unburned C II at this time. Note that we needed to include nonzero warping parameters in our fit to SYN++, indicating that the applied reddening correction is not exact.

Figure 4 displays our spectrum of SN 2014J after correction for only Milky Way extinction and for an assumed total $E(B - V) = 0.8$ mag, a spectrum of the SN Ia-norm SN 2011fe at very nearly the same phase ~ 7.5 d after first light (Parrent et al. 2012; Yaron & Gal-Yam 2012), and our best-fit SYN++ model. Comparing the spectra of these two SNe, and our SYN++ fit and those of SN 2011fe (Parrent et al. 2012), two major differences

appear: SN 2014J exhibits significantly less O II and C II absorption than SN 2011fe at the same phase, indicating that SN 2014J has very little unburned material in its atmosphere at 8.7 d, and SN 2014J shows strong evidence for high-velocity components in several species including Ca II and Si II. For now, we postpone any further spectral analysis.

4. CONCLUSIONS

In this *Letter* we present optical photometry and spectroscopy of the normal Type Ia SN 2014J. Despite the fact that it was found lamentably late for such a nearby SN, we show that existing pre-discovery observations of SN 2014J constrain the first-light time to be between Jan. 14.54 and 14.96, and we present Jan. 14.75 UT as our best estimate. In addition, the early-time light curve of SN 2014J does not match the canonical t^2 fireball model, instead exhibiting a variable power-law index similar to that derived for SN 2013dy. We look forward to further studies of this exciting object, and we hope that it will help us to better understand the underlying nature of SNe Ia.

A.V.F.'s group (and KAIT) at UC Berkeley have received financial assistance from the TABASGO Foundation, the Sylvia & Jim Katzman Foundation, the Christopher R. Redlich Fund, Gary and Cynthia Bengier, the Richard and Rhoda Goldman Fund, Weldon and Ruth Wood, and NSF grant AST-1211916. We thank the staffs at Lick Observatory and Itagaki Observatory where data were obtained.

REFERENCES

- Arnett, W. D. 1982, *ApJ*, 253, 785
Blondin, S., & Tonry, J. L. 2007, *ApJ*, 666, 1024
Branch, D., et al. 1994, *ApJ*, 421, 87
Cao, Y., et al. 2014, *The Astronomer's Telegram*, 5786, 1
Cardelli, J. A., Clayton, G. C., & Mathis, J. S. 1989, *ApJ*, 345, 245
Colgate, S. A., & McKee, C. 1969, *ApJ*, 157, 623
Cox, N. L. J., Davis, P., Patat, F., & Van Winckel, H. 2014, *The Astronomer's Telegram*, 5797, 1
Della Valle, M., & Melnick, J. 1992, *A&A*, 257, L1
Denisenko, D., et al. 2014, *The Astronomer's Telegram*, 5795, 1
de Vaucouleurs, G., et al. 1991, *Third Reference Catalogue of Bright Galaxies*
Filippenko, A. V. 1982, *PASP*, 94, 715
Filippenko, A. V. 1997, *ARAA*, 35, 309
Filippenko, A. V., Li, W. D., Treffers, R. R., & Modjaz, M. 2001, in *Small-Telescope Astronomy on Global Scales.*, ed. B. Paczyński, W. P. Chen, & C. Lemme (San Francisco: ASP), 121
Foley, R. J., et al. 2012, *ApJ*, 744, 38
Fossey, S. J., et al. 2014, *CBET*, 3792
Ganeshalingam, M., et al. 2010, *ApJS*, 190, 418
Goobar, A., et al. 2014, *arXiv:1402.0849*
Harris, G. L. H., Rejkuba, M., & Harris, W. E. 2010, *PASA*, 27, 457
Hillebrandt, W., & Niemeyer, J. C. 2000, *ARA&A*, 38, 191
Hoyle, F., & Fowler, W. A. 1960, *ApJ*, 132, 565
Karachentsev, I., & Kashibadze, O. G. 2006, *Astrophys.*, 49, 3
Li, W., et al. 2011, *Nature*, 480, 348
Ma, B., et al. 2014, *The Astronomer's Telegram*, 5797, 1
Miller, J. S., & Stone, R. P. S. 1993, *Lick Obs. Tech. Rep.* 66 (Santa Cruz: Lick Obs.)
Nugent, P. E., et al. 2011, *Nature*, 480, 344
Parrent, J. T., et al. 2012, *ApJ*, 752, 26
Perlmutter, S., et al. 1999, *ApJ*, 517, 565
Phillips, M. M., et al. 1992, *BAAS*, 24, 749
Piro, A., & Nakar, E. 2012, *arXiv:1211.6438*
Piro, A., & Nakar, E. 2013, *ApJ*, 769, 67
Polshaw, J., et al. 2014, *The Astronomer's Telegram*, 5816, 1
Poznanski, D., Prochaska, J. X., & Bloom, J. S. 2012, *MNRAS*, 426, 1465
Rabinak, I., Livne, E., & Waxman, E. 2012, *ApJ*, 757
Riess, A. G., Filippenko, A. V., Li, W., & Schmidt, B. P. 1999, *AJ*, 118, 2675
Riess, A. G., et al. 1998, *AJ*, 116, 1009
Sandage, A., & Tammann, G. A. 1975, *ApJ*, 196, 313
Sandage, A., et al. 1994, *ApJ*, 423, L13
Schlafly, E. F., & Finkbeiner, D. P. 2011, *ApJ*, 737, 103
Shappee, B. J., & Stanek, K. Z. 2011, *ApJ*, 733, 124
Silverman, J. M., et al. 2012a, *ApJ*, 756, L7
Silverman, J. M., et al. 2012b, *MNRAS*, 425, 1917
Stetson, P. B. 1987, *PASP*, 99, 191
Thomas, R. C., Nugent, P. E., & Meza, J. C. 2011, *PASP*, 123, 237
Yamanaka, M., et al. 2014, *arXiv:1401.5160*
Yaron, O., & Gal-Yam, A. 2012, *PASP*, 124, 668
Zheng, W., & Filippenko, A. V. 2014, *The Astronomer's Telegram*, 5828, 1
Zheng, W., et al. 2012, *ApJ*, 751, 90
Zheng, W., et al. 2013, *ApJ*, 778, L15 (Z13)

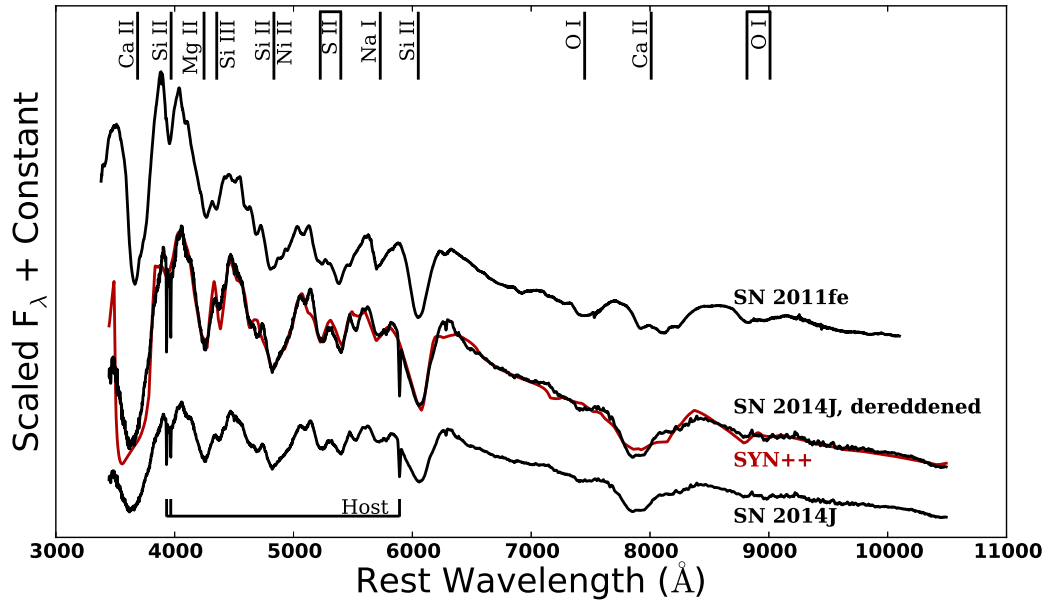


FIG. 4.— Spectrum of SN 2014J taken ~ 8.70 d after first light. The bottom spectrum shows SN 2014J after applying a reddening correction only for Milky Way dust. The middle spectrum displays SN 2014J after a reddening correction assuming a total $E(B - V) = 0.8$ mag, with our best SYN++ fit given in red. The top spectrum shows SN 2011fe at ~ 7.5 d after first light, for comparison (Parrent et al. 2012). Major spectral features are labeled at the top.